Excitation energy transfer in novel acetylenic perylene diimide scaffolds

David Shanks, Søren Preus, Katrine Qvortrup, Tue Hassenkam, Mogens Brøndsted Nielsen* and Kristine Kilså*

Received (in Durham, UK) 8th July 2008, Accepted 27th October 2008
First published as an Advance Article on the web 12th December 2008
DOI: 10.1039/b811565f

New perylene diimide (PDI) dimers (bis(PDI)s) with either tetraethynylethene (TEE) or 2,4-hexadiyne as the bridging unit were synthesized and the degree of intramolecular communication between the two PDI units was investigated as a function of the spacer unit and solvent polarity by absorption and emission spectroscopies, electrochemistry, and by atomic force microscopy (AFM). The experiments reveal that energy transfer occurs between TEE and PDI, and between PDI units. In the bis(PDI)-TEE system, flexible linkers allowed for intramolecular π–π stacking of the PDI chromophores in solution. The degree of stacking is solvent dependent, being more pronounced in non-polar solvents. The molecules were also found to self-assemble at a mica surface by intermolecular π–π interactions and to form fibrilar structures. Intermolecular excitation energy transfer was observed at the surface.

Introduction

Perylene diimides (PDI) have attracted wide interest as candidates for organic solar cells and artificial photosynthesis owing to their high fluorescence quantum yields and thermal chemical and photochemical persistency.[1–11] Much work has focused on controlling the ordering of perylene molecules by both rigid linkers as well as by self-assembly in order to favor the charge transfer and thus to improve the efficiency of photovoltaic cells.[12–17] We became interested in combining the field of PDI chemistry with the field of acetylenic scaffolding; the latter which has proven to be a very efficient tool for constructing large macromolecules[18–21] and thus, to develop new acetylenic derivatives of PDI. Acetylenic building blocks, for example silylated derivatives of di- and tetraethynylethene (TEE), have been successfully employed by Diederich and co-workers[19,21–25] for the construction of a large variety of conjugated molecules, such as poly(triacetylene) oligomers and expanded radialenes with interesting optical properties. In addition, TEE has been employed as a framework for organometallic species.[26–28] PDI-functionalized acetylenic building blocks are first steps towards larger arrays, for instance light-harvesting complexes. Here, we present the synthesis and photophysical investigation of TEE cores modified with one or two PDIs as well as two PDIs bridged by a 2,4-hexadiyne unit in order to extend our knowledge on aromatic π-stacking interactions that have been the subject of strong interest for decades.[29] Thus, the major aim is to elucidate how electronic communication between the two PDIs, such as ground-state π–π stacking or excimer formation, is influenced by the spacer and/or molecular structure, and to what degree the PDIs is electronically coupled to the central spacer. In addition, we have investigated the surface properties of these molecules by atomic force microscopy (AFM) in order to elucidate how the macroscopic morphology may change as a function of the spacer unit.

Department of Chemistry, University of Copenhagen, Universitetsparken, 5, DK-2100 Copenhagen Ø, Denmark. E-mail: mbn@kiku.dk. E-mail: kkj@nano.ku.dk

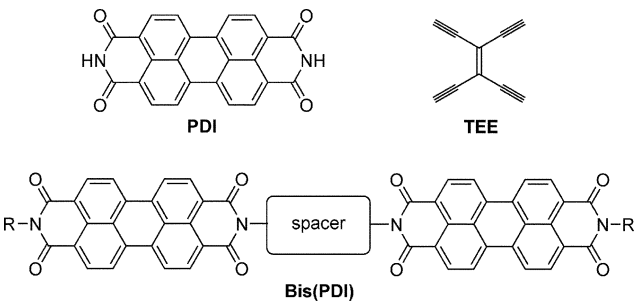

Results and discussion

Synthesis

First, a soluble bis(PDI) bridged by a 2,4-hexadiyne unit was prepared. *N*-(1-Hexylheptyl)perylene-3,4:9,10-tetracarboxylic 3,4-anhydride 9,10-imide **1** was prepared according to a literature protocol[6] and then condensed with propargyl amine in imidazole at 70 °C to afford the new and soluble acetylenic building block **2** in high yield (Scheme 1). This compound was then subjected to oxidative Hay homo-coupling[30] conditions to furnish the dimer **3** that was purified by precipitation from dichloromethane solution upon addition of methanol. The identity of the product, showing limited solubility, was supported by different spectroscopic means. While compound **2** shows sharp signals in its ^{1}H NMR spectrum, the spectrum of bis(PDI) **3** is characterized by rather broad signals when recorded in $CDCl_3$. The propargyl NCH_2 protons in compound **2** are observed as a sharp doublet at 4.99 ppm as they couple to the C≡CH proton, the signal of which is seen as a triplet at *ca.* 2.23 ppm, but overlapping a multiplet

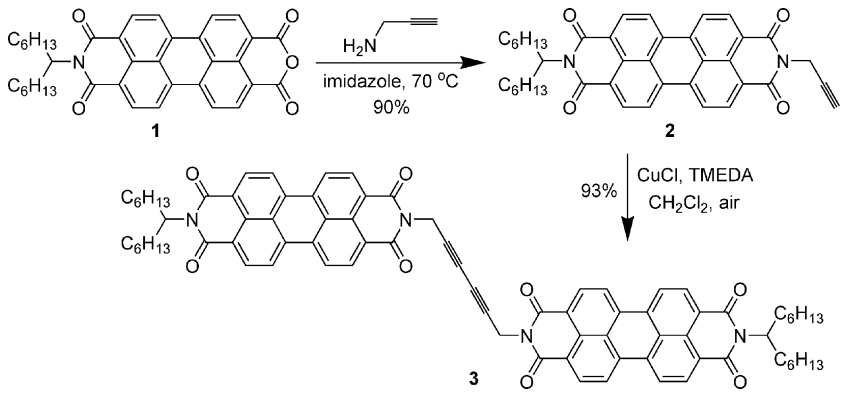

Scheme 1

originating from the 1-hexylheptyl groups. The assignment of these signals to neighboring NCH_2 and C≡CH groups was supported by a COSY spectrum. For compound **3**, the propargyl NCH_2 protons instead resonate as a broad singlet at 5.01 ppm as they do not any longer couple to other protons. The IR spectra of compounds **2** and **3** showed a clear difference in the region 3200–3300 cm^{-1}, the fingerprint region for the alkyne C–H stretch (Fig. 1); thus, compound **2** showed evident signals in this region that were absent in the spectrum of compound **3**. Finally, the structure **3** was supported by MALDI mass spectrometry.

For the synthesis of TEE-spaced dimers, we chose a final dicyclohexyl carbodiimide (DCC) promoted esterification reaction between a PDI containing a carboxylate group and geminally symmetrical TEEs incorporating two hydroxy functionalities. The latter TEE compounds were prepared by two-fold Sonogashira cross-coupling[31] reactions between the known dibromide **4**,[32] and terminal alkynes (Scheme 2). Hereby the new TEE building blocks **5** and **6** were obtained. Compound **5** (n = 1) was relatively unstable and was isolated in significantly lower yield.

The PDI **7** containing one carboxylic acid anchor group was prepared in almost quantitative yield by a condensation reaction between compound **1** and 4-aminobutyric acid at 130 °C in imidazole (Scheme 3), employing a slightly modified literature protocol.[6] Next, this carboxylic acid was treated

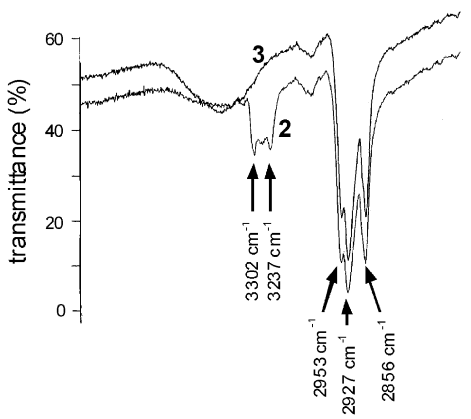

Fig. 1 Part of the IR spectra of compounds **2** and **3** (KBr pellets).

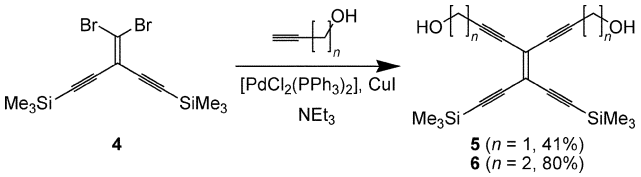

Scheme 2

with the TEE-alcohols **5** and **6**, respectively, in the presence of DCC to provide the two bis(PDI)s **8** and **9**. Moreover, we isolated the mono-coupled by-product **10** in a yield of 6%.

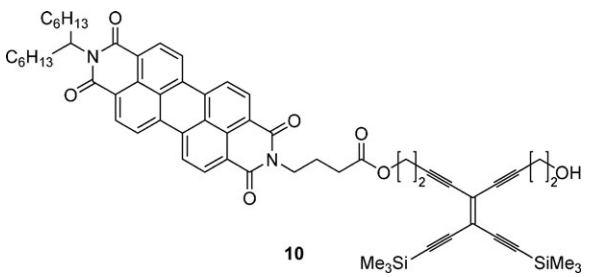

AFM surface studies

Compound **9** was subjected to morphology studies on dried mica surface using tapping mode AFM. The sample was prepared from toluene and subjected to both optical and atomic force microscopy. Under the optical microscope, the film did not reveal any significant structure apart from the ring structure created by the discontinuous receding of drop solvent during evaporation. AFM was used to study the area between the rings and the rings themselves. In the area between the rings, the molecules were in a disordered phase, while in the rings themselves the molecules apparently had more time (a matter of seconds) to form a more organized structure, as can be seen by the thread-like structure visible in the AFM images (Fig. 2). The fibrilar structure seen in the images does not seem to be made from bundles of identical single fibrils, but rather a complex structure with sheets of molecules with thin needles radiating out from a more complex center. The length of the fibrils is on the order of few hundred nanometers (100–400 nm), and the width of the smallest needles is on the order of 3–4 nm. However, due to the convolution effect in the image with the AFM tip, the true

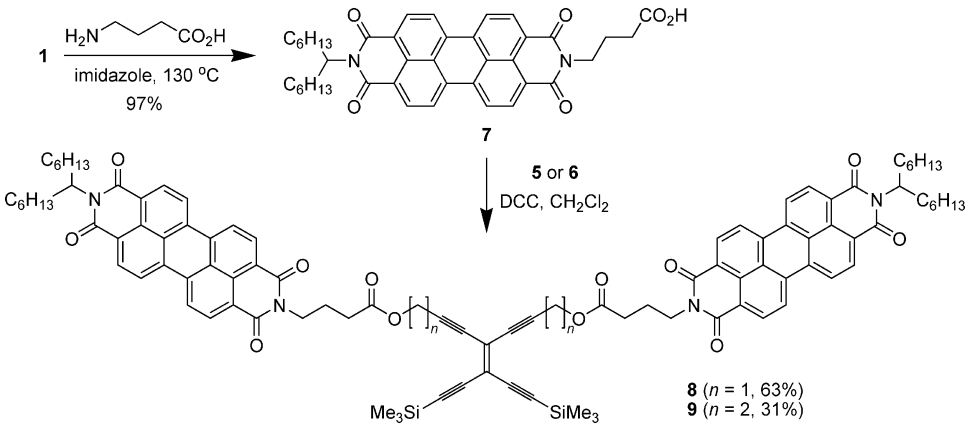

Scheme 3

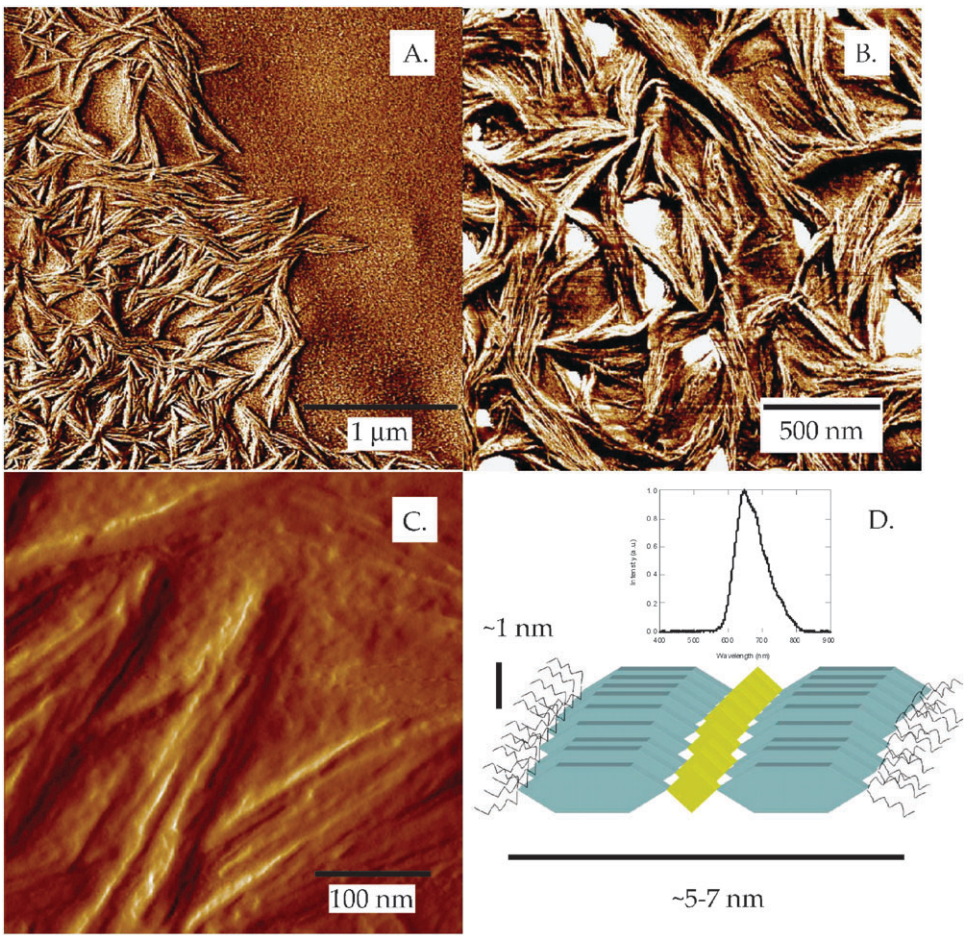

Fig. 2 AFM images of the surface of a dropcast film of compound **9**. (A) 3 × 3 µm AFM tapping mode phase image of a region close to the edge of the dropcast film, where there is a transition from a disordered phase into a thread like structure in the film. (B) 2 × 2 µm AFM tapping mode phase image of a region showing the structure of the thread like structure. (C) 500 × 500 nm AFM tapping mode amplitude image showing the structure of the individual threads. (D) Emission profile of the fibrils and a cartoon model showing an organization of the molecules that could give rise to the structure seen in the AFM.

width could be much smaller, and therefore the needles could very well be rows of stacked single molecules. This is also supported by the smallest thickness on the order of 1 nm of the sheets of material observed in some parts of the structure where there is no convolution problem. The sheets could therefore be molecules standing upright on their edges and stacked in one direction thus forming long rows of molecules giving rise to the structure seen in the AFM images. A schematic model of the assumed packing is shown in Fig. 2D. This motif is supported by X-ray analysis, which

reveals a π–π stacking distance of 3.4 Å between the PDIs, and by emission spectroscopy on the films which reveal a broad excimer-like emission (*vide infra*) indicative of strong coupling between PDIs (Fig. 2D).

The hexadiyne linked BisPDI **3** also forms fibrils at a mica surface, but with a much more complicated morphology.

Photophysical and electrochemical properties

TEE-coupled PDIs. The TEE coupled Bis(PDI)s (**8** and **9**) were subjected to photophysical investigations in various solvents and at various temperatures as well as to electrochemical studies. The properties are compared to suitable reference compounds, such as **6** and **11**, the latter being the methyl ester derivative of PDI **7**. Compound **8** ($n = 1$) behaves similarly to compound **9** ($n = 2$) and its properties will not be discussed further.

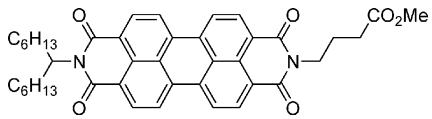

11

Fig. 3 shows the room-temperature absorption and emission spectra of compounds **6**, **9** and **10** in 2-methyltetrahydrofuran (MeTHF). The photophysical properties of the PDI unit have been characterized previously in numerous experiments.[6,33,34] Vibrational fine structure is clearly observed in the PDI S_0–S_1 transition at 450–550 nm. The S_0–S_2 transition is very weak, situated at 350–400 nm, and is most probably localized on the imide, as this transition is not seen in the unsubstituted perylene. The TEE absorption is located around 300–350 nm and is clearly visible and non-perturbed in compounds **9** and **10**. Only minor intrinsic absorptions (<10%) of PDI are found at these energies.

In PDI itself, and in the methyl ester reference compound **11**, the 0–0 transition is most intense, and the emission is the expected mirror image of the absorption. The change from a methyl group to a TEE unit (as in compound **10**) has only minor effects on the S_0–S_1 transition (larger spectral width and *ca.* 100 cm^{-1} bathochromic shift). The apparent change in the absorption spectra of the PDI vibrational fine structure between mono- and disubstituted TEE (**9** and **10**) is a consequence of electronic coupling of the two PDIs in **9** (*vide infra*).

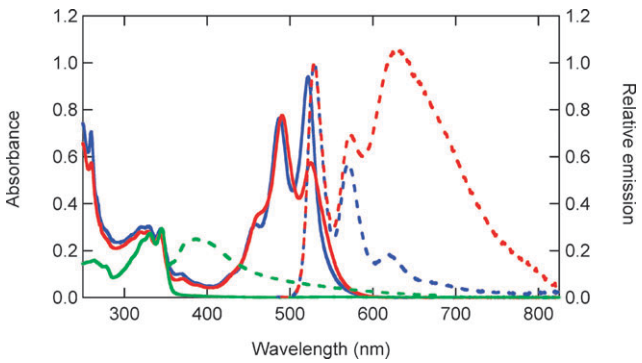

Fig. 3 Absorption (conc. ≈10 μM, solid, left) and emission (dashed, right) spectra of TEE **6** (green), **9** (red) and **10** (blue) in MeTHF.

The fluorescence quantum yield, ϕ_f, for **11** is high, but somewhat solvent dependent (CH_2Cl_2 (0.98) > PhMe (0.93) > MeCN (0.83) > MeTHF (0.74)). This is accompanied by a slight change in fluorescence lifetime, τ (4.2, 4.0, 4.1 and 3.8 ns, respectively), which yields a radiative rate constant, k_f, of 2.3–2.0 × 10^8 s^{-1}. The fluorescence quantum yield of **10** in various solvents is significantly lower than that of **11**, while the lifetimes are only slightly smaller; PhMe (ϕ_f/τ = 0.62/3.9 ns) > CH_2Cl_2 (0.59/3.8 ns) > MeCN (0.59/3.9 ns) > MeTHF (0.50/3.8 ns) yielding k_f of 1.6–1.3 × 10^8 s^{-1}. Within the series for one compound the differences correspond to the experimental uncertainty; however, some change in deactivation channels may be due to the larger structure in **10** facilitating more vibrational modes.

Focusing on MeTHF as solvent, it is clear from Fig. 3 that a spectral overlap can be found between TEE emission and PDI absorption. Thus, Förster type energy transfer[35] can take place in mono- and disubstituted TEEs from TEE to PDI, and we indeed observe an enhanced PDI emission when exciting into the TEE absorption band. As we are observing the acceptor emission, the energy transfer efficiency (ϕ_{EET}) can be found as $\phi_{EET} = ((F_A/F_A^0) - 1)(\varepsilon_A/\varepsilon_D)$, where F_A and F_A^0 are the integrated emission intensities for the acceptor with and without donor present, excited at the same wavelength. For both **9** and **10** this yields $\phi_{EET} \approx 0.2$. Using $\phi_{EET} = [1 + (r/R_0)^6]^{-1}$ this corresponds to a distance r = 24 Å between the two chromophores, as the critical Förster distance, R_0, for this pair of chromophores can be calculated to 19 Å.[35] Molecular mechanics simulations of **9** and **10** showed a very dynamic behavior of the chromophores at 300 K, and several local minima on the potential energy surface could be identified on account of the flexible nature of the linker. The distance between TEE and PDI in these simulations varied from 8–20 Å. Such dynamics simulations also suggested a disposition for the compound **9** to be in a folded state with a possibility for the two PDI units to be in a π-stacked conformation. AM1 semi-empirical quantum mechanical calculations[36] *in vacuo* of this local folded structure of **9** resulted in a stacked conformation and a distance between the two entities of 4 Å (not shown). Similar PM3 calculations of **9** resulted in a stacked-like conformation of the two PDIs exhibiting a slight relative rotational slipping and a slightly longer distance between the two entities of 5.0–5.4 Å (not shown). However, it is noted that π–π interactions are not encountered for in the semi-empirical calculations.[37]

Notably, the emission observed for **9** is a combination of monomeric and dimeric (excimer-like) emission. The dimeric emission is broad and structureless, and is similar to what can be observed for **11** in solid solution (MeTHF) at 77 K (data not shown) when excimers are formed. In addition, the absorption spectrum of **9** is also altered such that the (0–1) transition is higher in intensity than the (0–0) transition, and the spectrum is broadened and bathochromically shifted relative to that of **10**. These alterations are indicative of dimer formation in terms of π–π stacking and strong coupling of the PDI entities. Both H-type (parallel units) and J-type (rotational or lateral slipping of the units) stacking is expected to give similar spectral features. The pronounced alteration in absorption is mainly indicative of H-type attacking, while the

somewhat strong emission is indicative of a J-type stacking.[38] In the solid state only excimer-type emission was observed, thus, in the fibrils no PDIs are uncoupled to one another as no monomer type emission is seen (Fig. 2D).

In solution, the relative proportion of monomeric and dimeric emission is strongly dependent on excitation wavelength. Excitation spectra of **9** (77 K) recorded at two different emission wavelengths, 535 and 650 nm, are shown in the bottom part of Fig. 4. The structural features are similar to the absorption spectra of mono-PDI- and di-PDI-substituted TEE shown in Fig. 3. Resolving the spectra into monomer and dimer absorptions shows an equilibrium between stacked and non-stacked PDI units to be shifted strongly towards π–π stacked PDIs. There is no indication of this equilibrium to be significantly altered in the excited state.

In solid solutions at 77 K, the anisotropy of the TEE-coupled PDI also clearly reveals the strong coupling of the two PDI units. Compound **10** shows the expected anisotropy (r) for a perylene diimide[39] with r approaching 0.4 for the S_0–S_1 transition, indicative of almost parallel transition dipole moment directions for the emission and absorption. Negative anisotropy is found for the S_0–S_2 transition (imide related), although not as negative as for a purely perpendicular transition dipole moment. Excitation into the TEE absorption (≈300–350 nm) gives $r = 0$, in accordance with the energy transfer from TEE to PDI and the flexible nature of the linker.

The anisotropy of compound **9** is dependent on the emission wavelength, *i.e.*, monomeric or dimeric emission. The fluorescence excitation anisotropy recorded with $\lambda_{em} = 650$ nm is close to zero at all excitation wavelengths probably due to the delocalized nature of the excimer-type emission. At emission wavelengths where also the monomeric emission contributes ($\lambda_{em} = 535$ nm), the resulting anisotropy is a linear combination of the two limiting cases (Fig. 4).

Both the absorption and emission spectra of **9** are solvent dependent. Some selected examples are shown in Fig. 5, from which it is clear that dimer formation is much more pronounced in non-polar solvents such as toluene or MeTHF than it is in CH_2Cl_2 or $CHCl_3$. This could be due to π–π interactions of the PDIs, apparently favorable in non-polar solvents, or due to a more pronounced interaction between the imide groups and a polar solvent, thus shifting the equilibrium towards monomers in polar solvents. The order of increasing

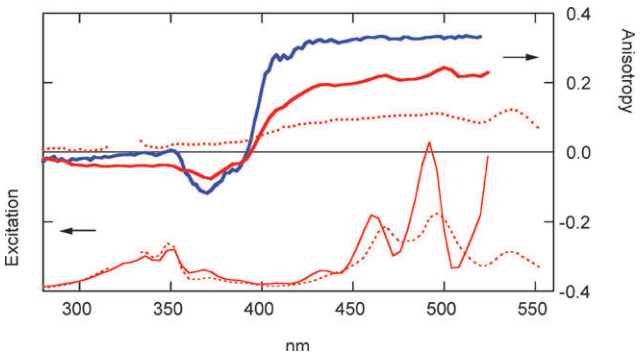

Fig. 4 Anisotropy of **10** (blue, $\lambda_{em} = 535$ nm) and **9** (red, $\lambda_{em} = 535$ nm (solid), $\lambda_{em} = 650$ nm (dotted)) in MeTHF (77 K). Also shown are the corresponding excitation spectra of **9** (thin lines).

dimer formation is $CHCl_3 < CH_2Cl_2 <$ PhMe $<$ MeTHF. However, there is no straight-forward correlation between the amount of dimer present and a simple solvent scale.

The lifetimes for the two emitting states of **9** measured in MeTHF were through a global analysis of time-correlated single photon counting data over a range of emission wavelengths found to be 3.8 ns (monomer-like) and 27.7 ns (dimer-like), respectively. The corresponding lifetimes are 3.6 and 28.7 ns in CH_2Cl_2. The spectral evolution in MeTHF is shown in Fig. 6. The lifetimes get slightly longer with decreasing temperature, but the effect is minimal (less than 10% from 300–100 K).

However, the emission profiles show an increase in the amount of dimer-like emission as the temperature decreases (Fig. 7). Both absorption and emission red-shift with decreasing temperature, except when the solvent (MeTHF) glasses and becomes rigid. In this case the emission blue-shifts again. In addition, we note that a shoulder is observed in the emission spectra as the temperature decreases.

As discussed above, the communication between the PDIs in **9** is more of a stacking nature on account of the flexible linker than an actual through-bond communication. The lack of through-bond communication is also borne out in the electrochemistry. Both **10** and **9** only show two reversible PDI reduction peaks at −1.05 and −1.22 V *vs.* ferrocenium–ferrocene (in CH_2Cl_2), which is similar to what has been found previously for perylene diimide derivatives.[40] The similarity between the mono- and di-linked systems suggests that in **9** both PDI units are reduced simultaneously.

Hexa-2,4-diyne linked PDI. Compound **3** is only sparingly soluble and has a strong tendency to form aggregates in MeTHF solution when more concentrated than 20 μM. The absorption and emission spectra of **3** at low concentration are similar to those of monomer PDI; there is no indication of π–π stacking or dimer formation. Semi-empirical PM3 geometry optimizations indicate that the smallest distance possible between the two PDI planes is 7.8 Å, N···N distance (Fig. 8), which is more than twice that of the optimum distance for the π–π stacking interaction. However, anisotropy measurements reveal a significantly lower ($r_{S0–S1} \approx 0.15$) anisotropy than found for the monomeric species, thus suggesting some interaction between the PDIs. Such an interaction is likely to be excitation energy transfer between PDIs, where a large spectral overlap of monomeric absorption and emission gives $R_0 = 52$ Å.

Experimental

General methods

Chemicals were purchased from Aldrich, Fluka, and GFS Chemicals and were used as received. THF was distilled from Na. Thin-layer chromatography (TLC) was carried out using aluminum sheets pre-coated with silica gel 60F (Merck 5554). Column chromatography was carried out using silica gel 60 (Merck 9385, 0.040–0.063 mm). Melting points were measured on a Reichert melting point apparatus equipped with a microscope and are uncorrected. ^{1}H NMR (300 MHz)

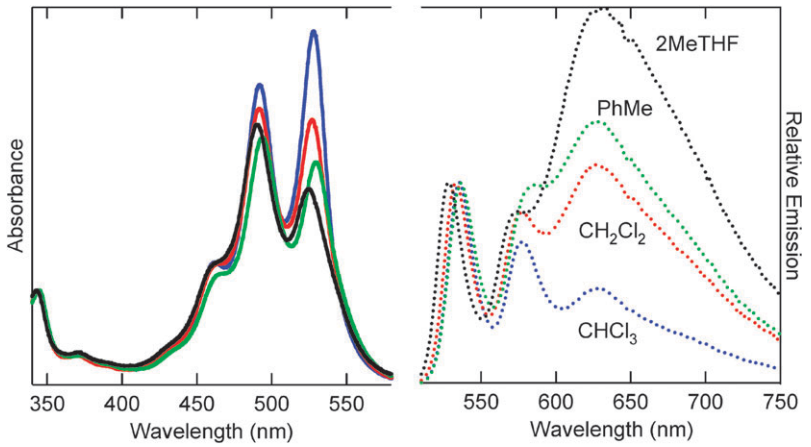

Fig. 5 Absorption spectra (left, solid) and emission spectra (right, dotted) of **9** in four different solvents: 2-methyl-THF (black), toluene (green), dichloromethane (red), and chloroform (blue). Emission spectra were acquired using an excitation wavelength of 460 nm.

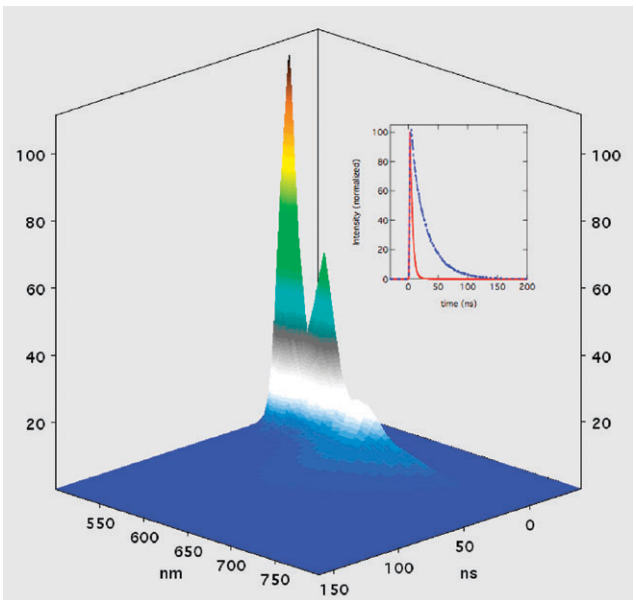

Fig. 6 Time resolved emission spectra of **9**, measured in MeTHF. Inset shows the measured kinetic profiles at 535 nm (red, solid) and 650 nm (blue, dashed) after excitation at 493 nm.

and ^{13}C NMR (75 MHz) spectra were recorded on a Varian instrument. Samples were prepared using $CDCl_3$ purchased from Cambridge Isotope Labs. Matrix-assisted laser-desorption/ionization time-of-flight mass spectrometry (MALDI–TOF–MS) was performed on a Bruker Autoflex instrument with dithranol as matrix. Fast atom bombardment (FAB) spectra were obtained on a Jeol JMS-HX 110 Tandem Mass Spectrometer in the positive ion mode using 3-nitrobenzyl alcohol (NBA) as matrix. Infrared (IR) spectra were obtained on a Bruker instrument. Microanalyses were performed at the Microanalytical Laboratory at the Department of Chemistry, University of Copenhagen.

For the photophysical measurements all solvents were used as received (Lab Scan, HPLC grade), except 2-methyl-tetrahydrofuran, MeTHF (Acros), which was distilled prior to use and stored over Na.

Steady state absorption and emission spectra at room temperature were recorded using a Cary 50 Bio UV/Vis and Fluorolog 3–22 (Jobin Yvon Horiba) spectrophotometer, respectively. Fluorescence quantum yields were measured relative to a *N*,*N*′-bis(1-hexylheptyl) PDI (Φ = 100% in $CHCl_3$).[41] Absorbances were kept below 0.1 at λ_{ex} to ensure linear response and to avoid inner filter effects. Fluorescence

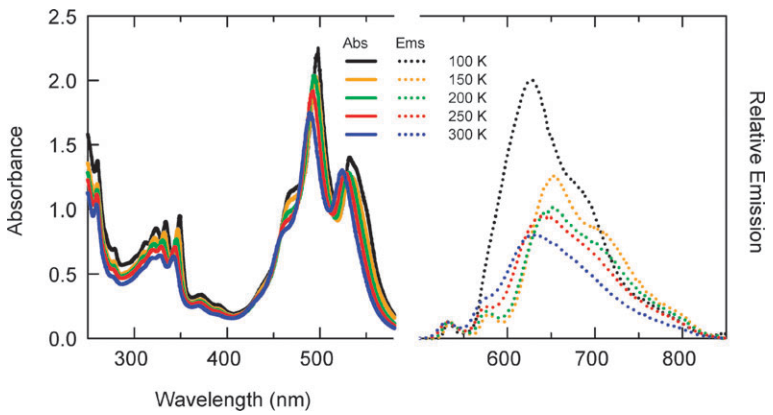

Fig. 7 Absorption (solid, left) and emission (dotted, right) of **9** in MeTHF from 300–100 K. Emission spectra were acquired using an excitation wavelength of 460 nm.

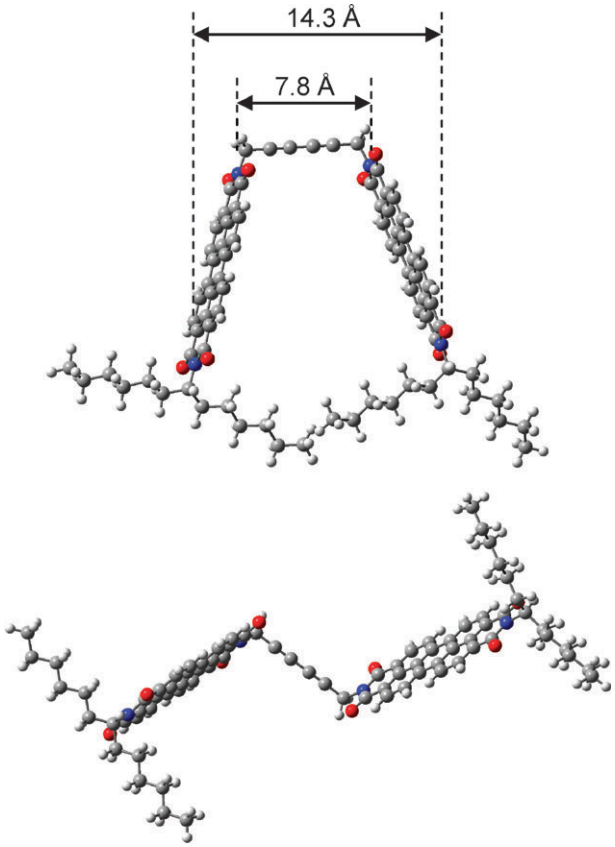

Fig. 8 Two conformations of compound **3** obtained by PM3 geometry optimization. The indicated distances are between two nitrogen atoms.

anisotropy was measured in vitrified 2-methyl-THF at 77 K using an Oxford optistatDN cryostat.

Time-correlated single photon counting data were measured by exciting at 493 nm using a NanoLED-495 (1 MHz repetition rate) and either a TBX-04 PMT equipped with suitable filters or a Hamamatsu R928 PMT after a monochromator in the above mentioned spectrophotometer. Data were analyzed and reconvoluted using DAS6 with a response function measured using a silica scatter solution. Time-resolved data were measured either up to 10 000 counts for fitting, or for 5 min at each wavelength for creating time-resolved emission spectra.

Cyclic voltammetry experiments were performed in dichloromethane (Labscan, HPLC grade, dried over molecular sieves) solutions containing 0.2 M Bu_4NPF_6 (from Aldrich, used as recieved) as supporting electrolyte, using a CHI630B potentiostat (CH Instruments, TX). A glassy carbon electrode was used as working electrode and a Pt wire was used as counter electrode, while the reference was Ag/Ag^+ in the same solvent. All potentials are reported relative to ferrocene (Fc^+/Fc, 0.31 V *vs.* SCE[42]) measured in the same setup.

Geometry optimizations were performed using Gaussian03.[43] Molecular dynamics simulations were performed in the absence of explicit solvent molecules using the Amber force field as implemented in the HyperChem program.[44] Temperature was set to 300 K and a distance dependent dielectric constant with a scale factor of 5 was applied in the calculations. Simulations were run for 100 ps with a time step of 0.001 ps.

Atomic force microscopy (AFM) was done on mica from drop-cast solutions in either $CHCl_3$ or toluene. Tapping mode was used to obtain pictures of the dried substrate using standard Olympus silicon tapping mode tips (TS160) with a resonant frequency of about 300 kHz. The instrument used was a Nanoscope IIIa from Veeco instruments.

The X-ray powder diffraction on compound **9** was done using a Stoe Stadi-P diffractometer utilizing Cu-Kα X-rays.

Preparation of the compounds

Compound 2. A mixture of **1** (100 mg, 0.17 mmol) and imidazole (250 mg) was ground to a homogenous powder using a glass rod. Under argon, propargylamine (100 μL, 0.7 mmol) was added by syringe, and the mixture was heated at 70 °C with stirring for 1 h. The mixture was then cooled to rt and dissolved in CH_2Cl_2. Celite (0.5 g) was added, the solvent was removed *in vacuo*, and the resulting "cake" was purified by column chromatography with direct deposition (gradient CH_2Cl_2 → CH_2Cl_2/*i*PrOH 95 : 5), yielding the product **2** as a dark red solid (96 mg, 90%). δ_H (300 MHz; $CDCl_3$) 8.69–8.55 (m, 8H), 5.19 (m, 1H), 4.99 (d, J = 3 Hz, 2H), 2.23 (overlapping m and t, 3H), 1.85 (m, 2H), 1.31 (m, 16H), 0.82 (t, J = 7 Hz, 6H); δ_C (75 MHz; $CDCl_3$) 162.7, 135.3, 134.3, 131.9, 131.3, 129.6, 126.7, 126.5, 123.5, 123.1, 122.9, 78.5, 70.9, 55.0, 32.5, 31.9, 29.7, 29.4, 27.1, 22.7, 14.2. IR (KBr): 3302, 3267, 3073 (br), 2953, 2927, 2856, 2123, 1931, 1699, 1659, 1595, 1579, 1507, 1482, 1455, 1434, 1404, 1378, 1366, 1251, 1217, 1194, 1173, 1136, 1126, 1107, 1006, 986, 913, 856, 833, 810, 795, 785, 746, 721, 668, 636. MALDI-MS: m/z 610.4 [M^-]. Found: C, 78.38; H, 6.42; N, 4.59. $C_{40}H_{38}N_2O_4$ requires: C, 78.66; H, 6.27; N, 4.59%.

Compound 3. Compound **2** (100 mg, 0.17 mmol) was dissolved in dry CH_2Cl_2 (40 mL), whereupon Hay catalyst (45 mg CuCl and 50 mg TMEDA dissolved in 1.5 mL CH_2Cl_2) was added. The mixture was stirred in an open flask overnight; as the reaction proceeds a red precipitate is observed. The mixture was washed with water and evaporated *in vacuo*. The resulting red solid was partly redissolved in CH_2Cl_2 (*ca.* 30 mL) and MeOH (*ca.* 50 mL) added. The resulting precipitate was collected by centrifugation, washed a few times with MeOH and dried *in vacuo* to give the product **3** (158 mg, 93%) as a red solid. δ_H (300 MHz; $CDCl_3$) 8.68–8.58 (m, 16H), 5.18 (m, 2H), 5.01 (s, 4H), 2.22 (m, 4H), 1.87 (m, 4H), 1.25 (m, 32H), 0.82 (t, J = 6 Hz, 12H); IR (KBr): 3077 (br), 2962, 2925, 2855, 1701, 1661, 1594, 1579, 1507, 1482, 1455, 1434, 1404, 1377, 1333, 1250, 1216, 1172, 1134, 1126, 1107, 983, 853, 833, 811, 796, 784, 746, 722, 666, 634; MALDI-MS: m/z 1218.8 [M^-]. Found: C, 77.81; H, 6.09; N, 4.65. $C_{80}H_{74}N_4O_8 \cdot H_2O$ requires C, 77.65; H, 6.19; N, 4.53%.

Compound 5. A solution of compound **4** (113 mg, 0.3 mmol) and NEt_3 (0.5 mL) in THF (5 mL) was degassed by argon bubbling and ultrasound for 1 h. To this solution, propargyl alcohol (53 μL, 0.9 mmol), $PdCl_2(PPh_3)_4$ (10 mg, 0.015 mmol), and CuI (6 mg, 0.03 mmol) were added, and the mixture was stirred overnight. The solvent was then removed *in vacuo* and

the resulting residue subjected to column chromatography (pentane–EtOAc 6 : 4) to give the product **5** as a brown solid (40 mg, 41%) that decomposes upon standing or heating. δ_H (300 MHz; $CDCl_3$) 4.46 (s, 4H), 2.16 (br s, 2H), 0.22 (s, 18H); δ_C (75 MHz; $CDCl_3$) 118.35, 118.31, 105.6, 100.7, 97.4, 82.6, 51.7, −0.2; MALDI-MS: m/z 328.7 [M + H^+].

Compound 6. A solution of compound **4** (113 mg, 0.3 mmol) and NEt_3 (0.5 mL) in THF (5 mL) was degassed by argon bubbling and ultrasound for 1 h. To this solution, 3-butyn-1-ol (68 μL, 0.9 mmol), $PdCl_2(PPh_3)_4$ (10 mg, 0.015 mmol), and CuI (6 mg, 0.03 mmol) were added, and the mixture was stirred overnight. The solvent was then removed *in vacuo* and the resulting residue subjected to column chromatography (pentane–EtOAc 6 : 4) to give the product **6** as a beige solid (85 mg, 80%). Mp 87 °C; δ_H (300 MHz; $CDCl_3$) 3.75 (t, J = 6 Hz, 4H), 2.68 (t, J = 6 Hz, 4H), 2.20 (br s, 2H), 0.21 (s, 18H); δ_C (75 MHz; $CDCl_3$) 119.3, 117.1, 104.3, 101.2, 97.2, 80.3, 60.7, 24.4, −0.2; HR-FAB-MS: m/z 356.1624 [M^+]; calc. for $C_{20}H_{28}O_2Si_2$: 356.1628. Found: C, 66.91; H, 7.92. $C_{20}H_{28}O_2Si_2$ requires C, 67.36; H, 7.91%.

Compound 7. A mixture of compound **1** (600 mg, 1.0 mmol), 4-aminobutyric acid (130 mg, 1.2 mmol), and imidazole (3 g) was ground to a homogenous powder using a glass rod. This mixture was then heated unstirred at 130 °C for 4 h. The mixture was then cooled to rt, suspended in EtOH (20 mL) and poured into 2 M aqueous HCl (150 mL). The resulting precipitate was collected by filtration, washed with water, and dried in the oven at 130 °C for 2 h to give the product **7** (674 mg, 97%) as a red solid. Mp >260 °C (lit.:[6] 307–308 °C); δ_H (300 MHz; $CDCl_3$) 8.56 (m, 8H), 5.16 (m, 1H), 4.29 (t, J = 6 Hz, 2H), 2.52 (t, J = 6 Hz, 2H), 2.30–1.20 (several peaks, 22H), 0.83 (t, J = 7 Hz, 6H); MALDI-MS: m/z 657.1 [M − H^+].

Compound 8. Dicyclohexylcarbodiimide (45 mg, 0.22 mmol) was added in a single portion to a slurry of the acid **7** (120 mg, 0.18 mmol), the propargylic diol **5** (30 mg, 0.09 mmol), and 4-dimethylaminopyridine (2 mg, 0.02 mmol) in dry CH_2Cl_2 (10 mL). The mixture was stirred at room temperature overnight, then the solvent was removed *in vacuo*. The residue was subjected to column chromatography (CH_2Cl_2–EtOAc–EtOH 94 : 5 : 1) to yield the product **8** (92 mg, 63%) as a deep red solid. Decomposed >160 °C; δ_H (300 MHz; $CDCl_3$) 8.52–8.38 (m, 16H), 5.18 (m, 2H), 4.83 (s, 4H), 4.26 (t, J = 7 Hz, 4H), 2.54 (t, J = 7 Hz, 4H), 2.20 (m, 8H), 1.88 (m, 4H), 1.34–1.24 (m, 32H), 0.83 (t, J = 6 Hz, 12H), 0.18 (s, 18H); δ_C (75 MHz; $CDCl_3$) 172.2, 163.3, 134.6, 134.1, 131.3, 129.5, 129.2, 126.24, 126.18, 123.1, 123.0, 122.9, 119.3, 117.7, 106.2, 100.4, 92.9, 83.1, 55.0, 52.7, 39.7, 32.5, 31.9, 31.8, 29.4, 27.1, 23.4, 22.7, 14.2, −0.2; MALDI-MS: m/z 1609.8 [M + H^-]. Found: C, 74.04; H, 6.53; N, 3.59. $C_{100}H_{104}N_4O_{12}Si_2\cdot(H_2O)_{0.5}$ requires C, 74.18; H, 6.54; N, 3.46%.

Compound 9. Dicyclohexyl carbodiimide (161 mg, 0.77 mmol) was added in a single portion to a slurry of the acid **7** (471 mg, 0.64 mmol), the diol **6** (30 mg, 0.32 mmol), and 4-dimethylaminopyridine (2 mg, 0.06 mmol) in dry CH_2Cl_2 (30 mL). The mixture was stirred at rt overnight, then the solvent was removed *in vacuo*. The residue was purified first by column chromatography (silica, CH_2Cl_2–EtOAc–EtOH 94 : 5 : 1), then gel permeation chromatography (Biobeads S-X1, CH_2Cl_2) to yield the product **9** (167 mg, 31%) as a red solid. Decomposed >200 °C; δ_H (300 MHz; $CDCl_3$) 8.46–8.15 (m, 16H), 5.15 (m, 2H), 4.26–4.20 (m, 8H), 2.81 (t, J = 7 Hz, 4H), 2.51 (t, J = 7 Hz, 4H), 2.25 (m, 4H), 2.13 (t, J = 7 Hz, 4H), 1.92 (m, 4H), 1.35–1.25 (m, 32H), 0.85 (t, J = 7 Hz, 12H), 0.20 (s, 18H); δ_C (75 MHz; $CDCl_3$) 172.7, 163.1, 134.2, 133.8, 131.5, 131.0, 129.3, 129.0, 125.9, 124.0, 123.3, 122.9, 122.8, 122.7, 119.8, 116.8, 104.3, 101.0, 96.0, 79.9, 62.0, 55.0, 39.8, 32.5, 32.0, 31.9, 29.4, 27.2, 23.4, 22.8, 20.5, 14.2, −0.1; MALDI-MS: m/z 1636.0 [M − H^+]. Found: C, 74.12; H, 6.60; N, 3.36. $C_{102}H_{108}N_4O_{12}Si_2\cdot0.5H_2O$ requires C, 74.38; H, 6.67; N, 3.40%.

Compound 10. Compound **10** was isolated as a by-product (21 mg, 6%) in the synthesis of compound **9**. δ_H (300 MHz; $CDCl_3$) 8.65–8.56 (m, 8H), 5.19 (m, 1H), 4.28–4.22 (m, 4H), 3.76 (t, J = 7 Hz, 2H), 2.78 (t, J = 7 Hz, 2H), 2.69 (t, J = 7 Hz, 2H), 2.49 (t, J = 7 Hz, 2H), 2.25 (m, 2H), 2.13 (t, J = 7 Hz, 2H), 1.87 (m, 2H), 1.23 (m, 16H), 0.83 (t, J = 7 Hz, 6H), 0.22 (s, 18H); δ_C (75 MHz; $CDCl_3$) 172.7, 163.6, 135.0, 134.5, 131.7, 131.4, 129.6, 128.1, 127.0, 123.4, 123.2, 119.8, 117.3, 104.7, 101.4, 101.0, 97.3, 96.1, 80.9, 79.8, 62.1, 60.8, 55.0, 39.8, 32.5, 31.9, 29.4, 27.1, 24.6, 23.5, 22.8, 20.6, 14.2, 0.0; MALDI-MS: m/z 995.6 [M − H^+].

Conclusion

Efficient synthetic protocols for acetylenic PDI scaffolds have been developed. These molecules are potential candidates for light harvesting arrays. The bis(PDI) system **3** with a rigid spacer does not allow for intramolecular π–π stacking of the two PDI units. Yet, anisotropy measurements do indicate some interaction between the PDIs, presumably excitation energy transfer between the PDI units. This compound was prepared by a successful Hay homo-coupling reaction of the terminal alkyne **2**. It will be interesting in future work to explore this same alkyne in reactions with azides using the Huisgen–Meldal–Sharpless reaction.[45–48]

In contrast, the flexible linker of the bis(PDI) system **9** allows for an intramolecular π–π stacking interaction, forming an intramolecular dimer of the two PDI units. This stacking seems to be present in both the ground and excited states and is promoted by nonpolar solvents, such as toluene and 2-methyltetrahydrofuran (Fig. 9). The relative amount of dimer-like emission increases with decreasing temperature. The interaction is, however, too weak to influence the electrochemical reduction of the PDI units, that is, they behave as independent redox centres reduced at the same potentials. Further, it was found that excitation energy transfer occurs from the TEE to the covalently attached PDI unit, which in the case of both mono- and disubstituted TEE occurs with an efficiency of $\phi_{EET} \approx 0.20$.

Both compounds **3** and **9** form fibrils at a mica surface, but with very different morphologies. For compound **9**, π–π stacking interactions seem to govern the global organization

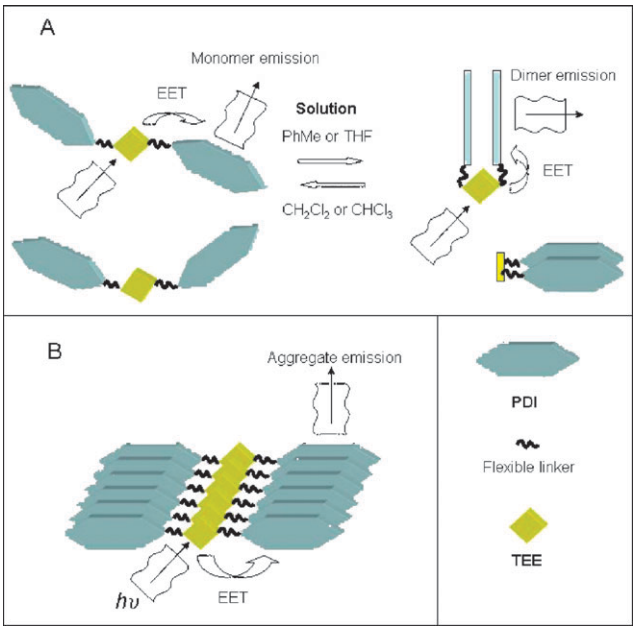

Fig. 9 Schematic summary of the photophysics of **9** in solution (A) and at a mica surface (B).

of the fibrils with intermolecular PDI–PDI distances of 3.4 Å; this stacking results in a broad excimer-like emission (Fig. 9).

Note added in Proof: Successful Huisgen-Meldal-Sharpless reactions (click reactions) on compound 2 were recently reported: M. Langhals and A. Obermeier, *Eur. J. Org. Chem.*, 2008 (Early View, Nov. 7).

Acknowledgements

We thank Niels Vissing Holst and Flemming Hansen for skillful technical assistance. The Carlsberg Foundation and the Danish Research Agency is acknowledged for financial support (grants #2111-04-0018 and #272-06-0017).

References

1 Y. J. Li, H. Y. Zheng, Y. L. Li, S. Wang, Z. Y. Wu, P. Liu, Z. Q. Gao and H. B. Liu, *J. Org. Chem.*, 2007, **72**, 2878–2885.
2 H. Z. Chen, M. M. Ling, X. Mo, M. M. Shi, M. Wang and Z. Bao, *Chem. Mater.*, 2007, **19**, 816–824.
3 N. Wang, Y. J. Li, X. R. He, H. Y. Gan, Y. L. Li, C. S. Huang, X. H. Xu, J. C. Xiao, S. Wang, H. B. Liu and D. B. Zhu, *Tetrahedron*, 2006, **62**, 1216–1222.
4 J. S. Wu, J. Q. Qu, N. Tchebotareva and K. Müllen, *Tetrahedron Lett.*, 2005, **46**, 1565–1568.
5 T. del Cano, V. Parra, M. L. Rodriguez-Mendez, R. Aroca and J. A. de Saja, *Org. Electron.*, 2004, **5**, 107–114.
6 H. Langhals and W. Jona, *Eur. J. Org. Chem.*, 1998, 847–851.
7 D. Schlettwein, D. Wohrle, E. Karmann and U. Melville, *Chem. Mater.*, 1994, **6**, 3–6.
8 K. Qvortrup, A. D. Bond, A. Nielsen, C. J. McKenzie, K. Kilså and M. B. Nielsen, *Chem. Commun.*, 2008, 1986–1988.
9 M. J. Ahrens, L. E. Sinks, B. Rybtchinski, W. Liu, B. A. Jones, J. M. Giaimo, A. V. Gusev, A. J. Goshe, D. M. Tiede and M. R. Wasielewski, *J. Am. Chem. Soc.*, 2004, **126**, 8284–8294.
10 B. Rybtchinski, L. E. Sinks and M. R. Wasielewski, *J. Am. Chem. Soc.*, 2004, **126**, 12268–12269.
11 T. van der Boom, R. T. Hayes, Y. Zhao, P. J. Bushard, E. A. Weiss and M. R. Wasielewski, *J. Am. Chem. Soc.*, 2002, **124**, 9582–9590.
12 V. Dehm, Z. J. Chen, U. Baumeister, P. Prins, L. D. A. Siebbeles and F. Würthner, *Org. Lett.*, 2007, **9**, 1085–1088.
13 P. Samori, A. Fechtenkötter, E. Reuther, M. D. Watson, N. Severin, K. Müllen and J. P. Rabe, *Adv. Mater.*, 2006, **18**, 1317–1321.
14 T. J. Tang, J. Q. Qu, K. Müllen and S. E. Webber, *Langmuir*, 2006, **22**, 26–28.
15 D. J. Yao, T. P. Bender, P. J. Gerroir and P. R. Sundararajan, *Macromolecules*, 2005, **38**, 6972–6978.
16 L. H. Gade, C. H. Galka, R. M. Williams, L. De Cola, M. McPartlin, B. Dong and L. F. Chi, *Angew. Chem., Int. Ed.*, 2003, **42**, 2677–2681.
17 G. Sui, J. Orbulescu, M. Mabrouki, M. Micic, R. M. Leblanc, S. G. Liu, R. A. Cormier and B. A. Gregg, *J. Phys. Chem. B*, 2002, **106**, 9335–9340.
18 *Acetylene Chemistry: Chemistry, Biology, and Material Science*, eds. F. Diederich, P. Stang and R. R. Tykwinski, Wiley-VCH, Weinheim, 2005.
19 M. B. Nielsen and F. Diederich, *Chem. Rec.*, 2002, **2**, 189–198.
20 M. B. Nielsen and F. Diederich, *Synlett*, 2002, 544–552.
21 F. Diederich, *Chem. Commun.*, 2001, 219–227.
22 M. B. Nielsen and F. Diederich, *Chem. Rev.*, 2005, **105**, 1837–1867.
23 J.-P. Gisselbrecht, N. N. P. Moonen, C. Boudon, M. B. Nielsen, F. Diederich and M. Gross, *Eur. J. Org. Chem.*, 2004, 2959–2972.
24 M. B. Nielsen, M. Schreiber, Y. G. Baek, P. Seiler, S. Lecomte, C. Boudon, R. R. Tykwinski, J.-P. Gisselbrecht, V. Gramlich, P. J. Skinner, C. Bosshard, P. Günter, M. Gross and F. Diederich, *Chem.–Eur. J.*, 2001, **7**, 3263–3280.
25 R. E. Martin, U. Gubler, C. Boudon, V. Gramlich, C. Bosshard, J.-P. Gisselbrecht, P. Günter, M. Gross and F. Diederich, *Chem.–Eur. J.*, 1997, **3**, 1505–1512.
26 R. Faust, F. Diederich, V. Gramlich and P. Seiler, *Chem.–Eur. J.*, 1995, **1**, 111–117.
27 O. F. Koentjoro, P. Zuber, H. Puschmann, A. E. Goeta, J. A. K. Howard and P. J. Low, *J. Organomet. Chem.*, 2003, **670**, 178–187.
28 M. I. Bruce, N. N. Zaitseva, P. J. Low, B. W. Skelton and A. H. White, *J. Organomet. Chem.*, 2006, **691**, 4273–4280.
29 For example, see: S. L. Cockroft, J. Perkins, C. Zonta, H. Adams, S. E. Spey, C. M. R. Low, J. G. Vinter, K. R. Lawson, C. J. Urch and C. A. Hunter, *Org. Biomol. Chem.*, 2007, **5**, 1062–1080, and references cited therein.
30 A. S. Hay, *J. Org. Chem.*, 1962, **27**, 3320–3321.
31 K. Sonogashira, Y. Tohda and N. Hagihara, *Tetrahedron Lett.*, 1975, 4467–4470.
32 J. Anthony, A. M. Boldi, Y. Rubin, M. Hobi, V. Gramlich, C. B. Knobler, P. Seiler and F. Diederich, *Helv. Chim. Acta*, 1995, **78**, 13–45.
33 H. Langhals, *Heterocycles*, 1995, **40**, 477–500.
34 H. Langhals, *Helv. Chim. Acta*, 2005, **88**, 1309–1343.
35 J. R. Lakowicz, *Principles of Fluorescence Spectroscopy*, 2nd edn, Springer, New York, 2004.
36 M. S. J. Dewar, E. G. Zoebisch, E. F. Healy and J. J. P. Stewart, *J. Am. Chem. Soc.*, 1985, **107**, 3902–3909.
37 J. J. P. Stewart, *J. Comput. Chem.*, 1989, **10**, 209–220.
38 H. Langhals and R. Ismael, *Eur. J. Org. Chem.*, 1998, 1915–1917.
39 C. Flors, I. Oesterling, T. Schnitzler, E. Fron, G. Schweitzer, M. Sliwa, A. Herrmann, M. van der Auwerer, F. de Schryver, K. Müllen and J. Hofkens, *J. Phys. Chem. C*, 2007, **111**, 4861–4870.
40 S. K. Lee, Y. B. Zu, A. Herrmann, Y. Geerts, K. Müllen and A. J. Bard, *J. Am. Chem. Soc.*, 1999, **121**, 3513–3520.
41 S. Demmig and H. Langhals, *Chem. Ber.*, 1988, **121**, 225–230.
42 A. J. Bard and L. R. Faulkner, *Electrochemical Methods: Fundamentals and Applications*, 2nd edn, John Wiley and Sons, Hoboken, NJ, 2001.
43 M. J. Frisch, G. W. Trucks, H. B. Schlegel, G. E. Scuseria, M. A. Robb, J. R. Cheeseman, J. A. Montgomery, Jr., T. Vreven, K. N. Kudin, J. C. Burant, J. M. Millam, S. S. Iyengar, J. Tomasi, V. Barone, B. Mennucci, M. Cossi, G. Scalmani, N. Rega, G. A. Petersson, H. Nakatsuji, M. Hada, M. Ehara, K. Toyota, R. Fukuda, J. Hasegawa, M. Ishida, T. Nakajima, Y. Honda, O. Kitao, H. Nakai, M. Klene, X. Li, J. E. Knox, H. P. Hratchian, J. B. Cross, V. Bakken, C. Adamo, J. Jaramillo, R. Gomperts, R. E. Stratmann, O. Yazyev, A. J. Austin, R. Cammi, C. Pomelli, J. Ochterski, P. Y. Ayala, K. Morokuma, G. A. Voth, P. Salvador, J. J. Dannenberg, V. G. Zakrzewski, S. Dapprich, A. D. Daniels, M. C. Strain,

O. Farkas, D. K. Malick, A. D. Rabuck, K. Raghavachari, J. B. Foresman, J. V. Ortiz, Q. Cui, A. G. Baboul, S. Clifford, J. Cioslowski, B. B. Stefanov, G. Liu, A. Liashenko, P. Piskorz, I. Komaromi, R. L. Martin, D. J. Fox, T. Keith, M. A. Al-Laham, C. Y. Peng, A. Nanayakkara, M. Challacombe, P. M. W. Gill, B. G. Johnson, W. Chen, M. W. Wong, C. Gonzalez and J. A. Pople, *GAUSSIAN 03 (Revision B.03)*, Gaussian, Inc., Wallingford, CT, 2004.

44 Hyperchem Hybercube, Inc., 2002.
45 R. Huisgen, G. Szeimies and L. Moebius, *Chem. Ber.*, 1967, **100**, 2494–2507.
46 R. Huisgen, *Pure Appl. Chem.*, 1989, **61**, 613–628.
47 C. W. Tornøe, C. Christensen and M. Meldal, *J. Org. Chem.*, 2002, **67**, 3057–3064.
48 V. V. Rostovtsev, L. G. Green, V. V. Fokin and K. B. Sharpless, *Angew. Chem., Int. Ed.*, 2002, **41**, 2596–2599.

